

Biophysical properties of the extra-cellular domain of the calcium-sensing receptor

Zachary C. Ryan ^a, Theodore A. Craig ^b, Sergei Yu. Venyaminov ^{c,d},
James R. Thompson ^a, Rajiv Kumar ^{b,c,*}

^a Department of Physiology and Biomedical Engineering, Mayo Clinic, Rochester, MN, USA

^b Department of Internal Medicine, Mayo Clinic, Rochester, MN, USA

^c Department of Biochemistry and Molecular Biology, Mayo Clinic, Rochester, MN, USA

^d Department of Molecular Pharmacology and Experimental Therapeutics Mayo Clinic, Rochester, MN, USA

Received 31 July 2006

Available online 17 August 2006

Abstract

The Calcium-Sensing Receptor (CaSR) is a G-protein-coupled receptor that regulates calcium homeostasis by altering parathyroid hormone release, and which binds divalent and trivalent cations, amino acids, polyamines, and polycationic ligands. To obtain information about the structural properties of the CaSR, we expressed milligram quantities of a pure, homogeneous, and functional fragment of the human CaSR extracellular domain (residues 20–535). The expressed and purified protein is folded and binds both neomycin and calcium. It forms dimers in the absence of reducing agents such as β -mercaptoethanol. Thermal denaturation studies show it has enthalpy and entropy values of unfolding equal to $\Delta H = -178 \pm 4$ kJ/mol and $\Delta S = -535 \pm 13$ J/mol/K. The protein has significant secondary structure with α -helical, β -sheet, β -turns, and disordered content of $36.6 \pm 6.7\%$, $13.3 \pm 5.3\%$, $20.2 \pm 3.3\%$, and $29.4 \pm 4.0\%$, respectively. The described method for the expression and purification of CaSR should prove useful for further structural studies of this physiologically important protein.

© 2006 Elsevier Inc. All rights reserved.

Keywords: Calcium-sensing receptor; G-protein-coupled receptor; Calcium; Secondary structure; Stability

The calcium-sensing receptor (CaSR) is a G-protein-coupled receptor (GPCR) which regulates calcium homeostasis via regulation of parathyroid hormone secretion [1–5]. Ca^{2+} binds to the receptor and inhibits PTH secretion [1–5]. Inactivating mutations of the CaSR are associated with and result in the hypercalcemic disorders, familial hypocalciuric hypercalcemia (FHH), and neonatal severe hyperparathyroidism (NSHPT) [2,3,5,6]. Activating mutations are responsible for autosomal dominant hypocalcemia with hypercalciuria (ADHH) and Bartter's syndrome type V [3–5]. The CaSR is expressed in several cell types sensitive to calcium modulation other than the parathyroid, such as neurons [7,8], cardiac myocytes [9],

kidney epithelial cells [10], and various other epithelia [11–13]. It has been shown to bind various di- and trivalent cations, amino acids, polyamines, and several antibiotics [2,14]. The CaSR also appears to have many functions outside of calcium regulation, involving programmed cell death, hormone regulation, cell proliferation, ion channel regulation, and gene expression [2–5].

Studies of the biophysical properties of the CaSR such as secondary and tertiary structure, metal binding properties, and binding to other ligands have been hampered by the absence of large amounts of pure receptor. In the present study, we describe a method for the expression and purification of chemically homogeneous, soluble CaSR extracellular domain (CaSR ECD). CaSR was expressed in insect cells as a secreted protein and was purified using a combination of metal-affinity chromatography and neomycin-affinity chromatography. The expressed receptor is

* Corresponding author. Fax: +1 507 538 3954.

E-mail address: rkumar@mayo.edu (R. Kumar).

folded, has significant α -helical and β -sheet structure, and binds both calcium and neomycin.

Materials and methods

General. Protein sequencing was carried out as described earlier [15–17]. DNA sequencing and oligonucleotide synthesis were performed using an automated DNA sequencer and an oligonucleotide synthesizer, respectively [18–21] (Applied Biosystems, Foster City, CA). Protein concentrations were determined using the BioRad Protein Reagent (Bradford) method [22] (Bio-Rad Laboratories, Hercules, CA) and the BCA Reagent with bovine serum albumin as the standard (Pierce Biochemicals, Rockford, IL) and by measuring UV absorbance. SDS–PAGE was carried out using an XCell II apparatus (Invitrogen, Carlsbad, CA) or by using a Phastgel apparatus (GE Healthcare, Piscataway, NJ). Reagents were from Sigma-Aldrich (St. Louis, MO) unless otherwise noted.

Molecular cloning. The extracellular domain of the human CaSR lacking signal peptide and the cysteine-rich domain (Tyr20–Arg535) was expressed in *Trichoplusia ni* insect cells (Invitrogen) utilizing a pIB/V5-His vector, which contains C-terminal V5 and histidine tags. A 5' oligonucleotide complementary to the chosen cDNA sequence of the CaSR ECD contained a Kozak consensus sequence and a melittin secretory signal: (5'-GAGAAAGCTTGCCATGAAATCTTAGTCAACGTTGCCCTGT TTTTATGTCGTATACATTTCTTACATCTATGCCTACGGGCC ATCCAGCGAGCCCA-3'). The 3' oligonucleotide complementary to chosen CaSR sequence also contained a PreScission protease (GE Healthcare) sequence: (5'-GAGACTCGAGGTGGGCCCCCTGGAACAG AACTTCCAGCCTGGAGAACCCACTCCACAGGAT- 3'). Oligonucleotides were used to amplify the selected CaSR sequence by standard PCR methods [23]. The PCR product was ligated into pIB/V5-His (Invitrogen) and the chimeric plasmid was used to transform *Escherichia coli* TOP10 cells (Invitrogen). Colonies were screened for the presence of plasmids containing the PCR product. The DNA sequence of the inserts was verified using dideoxy sequencing methods [21]. Appropriate clones were used for transfection of insect cells as described below.

Cell growth and expression. CaSR ECD (amino acid residues 20–535) in pIB-V5-His (Invitrogen) containing a melittin secretion signal was transfected into BT1-TN-5B1-4 HighFive™ (*Trichoplusia ni*) cells (Invitrogen) using cellfectin reagent (Invitrogen). Cells were screened for positive transfection with 50 μ g/mL Blasticidin S (Invitrogen) and anti-V5-HRP antibody (Invitrogen), and were grown in T175 flasks (Falcon). This process was repeated six times with increasing amounts of Blasticidin S (60–240 μ g/mL) to achieve optimal recombinant protein expression. 300 mL of Express Five® SFM medium (Invitrogen) containing 2 mM L-glutamine (Invitrogen) and 50 μ g/mL Blasticidin were seeded to a density of 5×10^5 cells/mL in a 2 L flask, and incubated in an Innova 55 R (New Brunswick Scientific) platform incubator at 27 °C, 120 rpm rotation speed. After the cell density reached 5×10^6 cells/mL, aliquots of the medium were used to inoculate ~850 mL of insect cell medium [24] in 2 L flasks to a density of 1.5×10^5 cells/mL. Flasks were incubated at 27 °C in a shaking platform incubator at a speed of 150 rpm.

Cell harvesting and protein purification. When a cell density of 5×10^6 cell/mL was reached (approximately 10 days), cells were harvested by centrifugation at $1500 \times g$ for 30 min. The supernatant was filtered through a 0.22 μ m filter (Millipore, Billerica, MA) and concentrated to a volume of approximately 600 mL using a ProFlux tangential flow concentrator (Millipore), with two 10,000 molecular weight cut-off YM membrane cartridges in series. To the concentrated medium, 3 L of Buffer A (20 mM sodium phosphate, pH 7.1, 500 mM sodium chloride) was added and the diluted medium was concentrated again to 600 mL by tangential flow. This process was repeated four times. The concentrated protein was collected and the concentrator was washed with 1 L Buffer A. This wash was combined with the original concentrate, and the total volume was filtered through a 0.22 μ m filter. The concentrated, dialyzed, and filtered medium was applied to a 16/10 HisPrep HP column (GE Healthcare) pre-equilibrated with Buffer A, using an AKTA FPLC (GE Healthcare) Sample Pump P-950 at a flow rate of 5 mL/min. A non-linear,

segmented gradient of 0–100% Buffer B (20 mM sodium phosphate, pH 7.1, 500 mM sodium chloride, and 500 mM imidazole) was run using a buffer volume of 1000 mL at a flow rate of 5 mL/min. Fractions were analyzed by Western blot, using an anti-V5-HRP antibody (Invitrogen) and SDS–PAGE followed by Coomassie blue staining of gels. Fractions showing both signal from Western analysis, and relative purity on Coomassie staining, were pooled and dialyzed into Buffer C (5 mM sodium phosphate, pH 7.1, 100 mM sodium chloride) using SpectraPor 6 dialysis tubing (molecular weight cut-off 1000 D, Spectrum Industries, Rancho Dominguez, CA). Following dialysis, pooled fractions were concentrated to 1 mL using a CentriPrep YM-50 (Millipore). This was applied to a constructed neomycin-Sepharose 4B column [25] using an AKTA FPLC at a flow rate of 3 mL/min. The neomycin column was synthesized by adding 30 mg of neomycin to 5 g of cyanogen bromide-activated Sepharose 4B. The material was then packed into an XK16 column (GE Healthcare) for chromatography. Protein was eluted during a non-linear, segmented gradient of 0–100% Buffer D (300 mM sodium phosphate, pH 7.1, 100 mM sodium chloride) over the course of 1000 mL at a flow rate of 3 mL/min. Fractions were again analyzed by Western blot, using an anti-V5-HRP antibody. Selected fractions were pooled, concentrated with a CentriPrep YM-50, and analyzed by SDS–PAGE for purity. Typical yield at this point is approximately 1–2 mg.

Concentration determination. Measurements in the near UV range were done using a DU 640 spectrometer (Beckman Instruments, Fullerton, CA) with a spectral bandwidth of 1.8 nm, and employing the CaSR ECD molar absorptivity of $77.0 \pm 1.5 \text{ mM}^{-1} \text{ cm}^{-1}$ at 281 nm obtained by averaging the results from four methods of calculation [26–29]. All spectra were corrected for turbidity by plotting the dependence of the log of the absorbance of the solution versus the log of the wavelength and extrapolating the linear dependence between these quantities in the range 340–440 nm to the absorption range 240–300 nm. The extrapolated values of absorbance were then subtracted from the measured value, and these corrections decreased the apparent absorbance of protein at 281 nm by about 17%. The scatter correction routine of the DU-640 was used for this purpose.

Circular dichroism spectroscopy. CD spectra of apo-CaSR in 20 mM sodium phosphate, 0.1 M NaCl, pH 7.2, were collected on a J-810 (JASCO, Japan) spectropolarimeter continuously purged by N₂ and equipped with a temperature control system CTC-345. Spectral and temperature dependent measurements were performed at a bandwidth of 2 nm using a U-type quartz cell of path length 0.148 mm (far-UV, 186–250 nm) and at bandwidth 1 nm using a rectangular 0.5 cm quartz cell (near-UV, 250–320 nm) in a homemade thermostated cell holder. CD spectra were recorded using five accumulations, each at scan speed of 20 nm/min and response time of 2 s. CD spectra were collected at 10 °C. The continuous temperature dependence of the ellipticity at 226 nm was measured using a scan rate of 50 °C/h and a response time of 8 s. Solvent evaporation was prevented by placing a drop of oil (that had been repeatedly boiled in water to remove soluble impurities) on the top of the sample in the cell. Far-UV CD spectra were smoothed by a JASCO noise reduction routine. The midpoint of heat denaturation was taken as a position of the maximum for the first derivative of the experimental melting curve. The van't Hoff enthalpy and entropy changes upon heat denaturation were calculated by the “Denatured Protein Analysis” program (J-810 software). CD data are presented in units of molar ellipticity per residue. Secondary structure of CaSR ECD was calculated from CD spectra in the far-UV spectral range using the CDPro suite of programs [30]—a modified version of three methods: SELCON3 [31], CONTIN/LL–CONTIN method [32] in locally linearized approximation [33], and CDSSTR [34]. In addition to the secondary structure content, programs in the CDPro package also calculate the number and average length of the secondary structure segments. The number of the secondary structure segments is calculated by dividing the number of residues included in the distorted helical structure by factor of four and in the distorted β structure by factor of two. Dividing the total amount of residues in α -helix or β -strand (ordered plus disordered) by the number of segments gives the average length of the segment. Tertiary structure class was determined by the Cluster program [35] of CDPro. Two sets of reference proteins were used for secondary structure

calculation: 48 proteins [36], or 23 $\alpha + \beta$ reference proteins, which were selected by the Cluster program.

Fluorescence titration. The CaSR fluorescence titrations at concentration of $\sim 3 \mu\text{M}$ were performed at room temperature in 20 mM Hepes, 0.1 M NaCl, 10 μM EGTA, pH 7.7, by adding known amount of CaCl_2 . The corrected fluorescence emission (excitation at 295 nm) spectrum from 300 to 500 nm was collected with a Fluorolog 3 (Jobin Yvon, France). Because the shape of fluorescence spectra did not change at different calcium concentrations, the relative fluorescence at 343 nm (position of maximum) was plotted, after correction for protein dilution, during titration as function of total calcium concentration.

Results and discussion

CaSR ECD is purified to homogeneity, binds neomycin, calcium, and forms dimers in the absence of reductant

His-tagged CaSR ECD was efficiently separated from other proteins present in the insect cell incubation medium with a HisPrep 16/10 column (Fig. 1) using an imidazole gradient. Approximately 3 mg of CaSR ECD is routinely isolated with greater than 95% purity from 10 L insect cell medium following a single cycle of nickel affinity chromatography. Fractions containing the CaSR ECD were concentrated and the concentrate was applied to a neomycin-Sepharose 4B column synthesized as described in the methods. Approximately 1.5 mg of CaSR ECD was recovered in pure form following application of approximately 3 mg of starting material (Fig. 2). Neomycin was chosen both as a purification step and a potential method for iso-

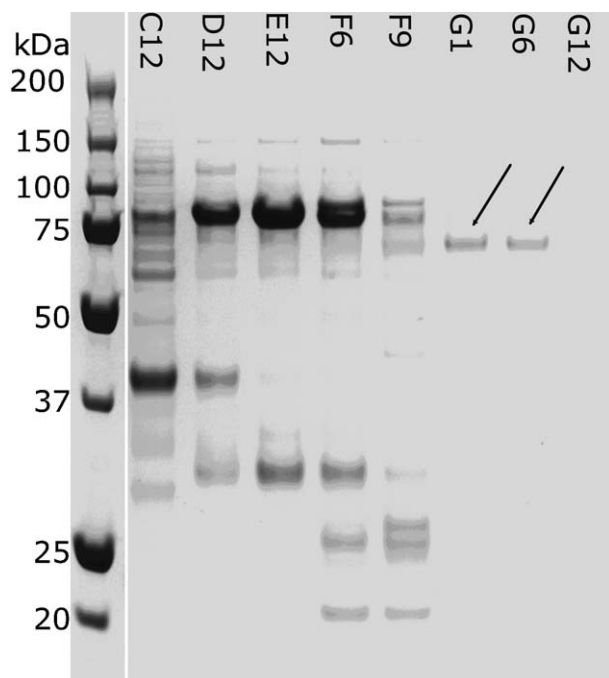


Fig. 1. Coomassie blue stained SDS-PAGE gel of fractions from the HisPrep 16/10 column purification. This typical elution profile shows that CaSR ECD elutes primarily around fractions G1–G6 (diagonal lines) after most non-specifically binding proteins have eluted from the column. This mostly pure CaSR elutes from the column at roughly 200 mM imidazole beginning at Fraction G1 on this Coomassie stained SDS-PAGE gel.

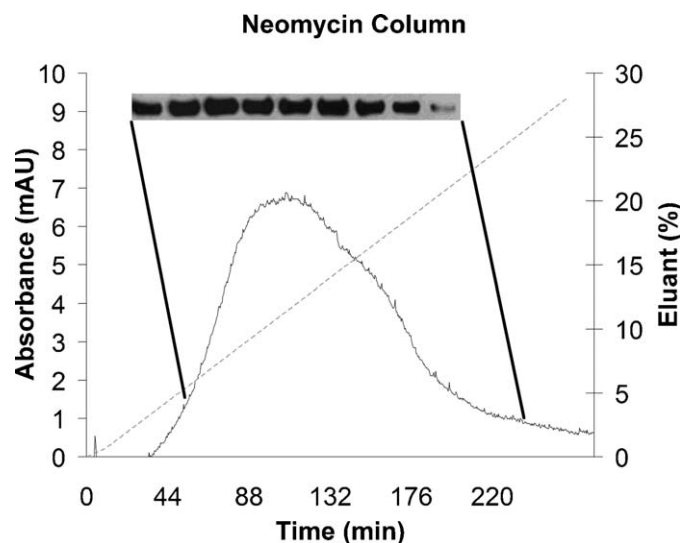


Fig. 2. Chromatography of CaSR ECD on a neomycin-Sepharose 4B column. Full length CaSR ECD elutes from the column predominantly in fractions A12 through D12. Corresponding Western analysis confirms these fractions contain homogeneous CaSR ECD (shown in insert). Solid line (—) UV absorbance at 280 nm. Dashed line (---) percent buffer D (see Materials and methods).

lating natively folded, bioactive protein, due to the well-documented ability of CaSR ECD to bind neomycin [2,14]. Selected fractions from the neomycin column were pure as determined by SDS-PAGE under reducing and non-reducing conditions (Fig. 3). The reduced sample treated with 10 mM DTT prior to gel loading has a M_r of approximately 70,000 (lane A), very close to the predict-

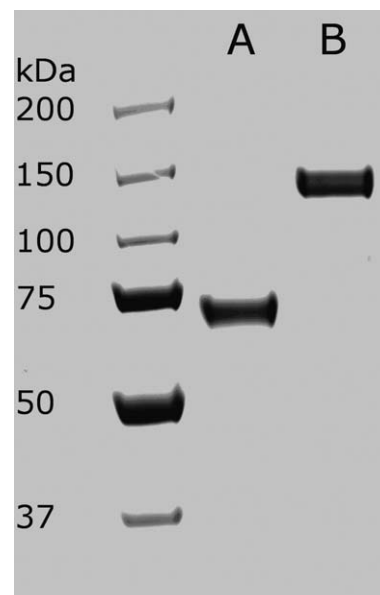


Fig. 3. SDS-PAGE of purified CaSR ECD under reducing and non-reducing conditions. (Lane A) CaSR ECD in the presence of 10 mM DTT. (Lane B) CaSR ECD without reductant. Samples were otherwise treated identically prior to gel loading. The molecular weight is indicated by Broad Range markers (Bio-Rad).

ed molecular mass of 64 kDa. The non-reduced sample shows a M_r of 140,000, compatible with dimerization of the receptor extracellular domain (lane B). A corresponding Western blot using anti-V5-HRP antibody confirms these results (data not shown). The identity of the CaSR extracellular domain was confirmed by mass spectrometry of tryptic digests of the purified protein.

Fluorescence titration

Addition of Ca^{2+} to apo-protein in Hepes buffer leads to progressive quenching of tryptophan fluorescence at 343 nm (data not shown). The overall decrease in fluorescence intensity is 62% of the original value without changes in the wavelength of emission maximum in the range of Ca^{2+} concentration 0–8 mM. CaSR ECD has a midpoint on the titration curve at $[\text{Ca}^{2+}] \approx 1.4$ mM. This affinity is compatible with the affinity of full-length receptor for Ca^{2+} in vivo [2,3,5] and is appropriate for sensing changes in serum calcium levels.

CaSR ECD is folded

Fig. 4A shows the far-UV CD spectrum of CaSR ECD in the apo-state. It has positive a maximum at 193 nm, a cross-over point at 200.5 nm, and two minima at 208 and 226 nm. The shape and amplitude of this spectrum are characteristic for proteins with a significant content of helical structure.

We used the CDPro suite of three programs [30] for estimation of the secondary structure and employed two sets of reference proteins: 48 proteins [31] or 23 $\alpha + \beta$ reference proteins, which were selected by the Cluster program [35]. The values shown in Table 1 are averages from six calculations for each type of secondary structure. The RMS deviations in Table 1 do not demonstrate real error for estimated values of secondary structure but rather the scattering of results for three methods of calculation and two sets of reference proteins. The calculations suggest that $\sim 70\%$ of the amino acid residues of CaSR ECD have ordered secondary structure (α -helices, β -strands, and turns). As shown in Table 1, 204 ± 22 of 557 residues of CaSR ECD ($\sim 37\%$ are included in 19–24 helical segments with average length of 9–10 residues), 74 ± 29 residues ($\sim 13\%$) are in β sheet (14–23 strands with average length of 4–5 residues), ~ 112 residues ($\sim 20\%$) are in turns, and ~ 164 residues (29.4%) are in unordered structure. The sequences of the 6 \times His and V5 tags as well as additional linker amino acids are included in this analysis. A Cluster analysis of the CD spectrum in Fig. 4A shows CaSR ECD belongs to a protein family with an $\alpha + \beta$ class of tertiary structure [35].

CD spectra in the near-UV spectral range are shown in Fig. 4B. The peaks at ~ 261 and ~ 268 nm are attributed to the L_b transition of phenylalanine (PHE), and peaks at ~ 283 and ~ 293 nm to the L_b transition of tryptophan (TRP). All these peaks are negative. The broad positive

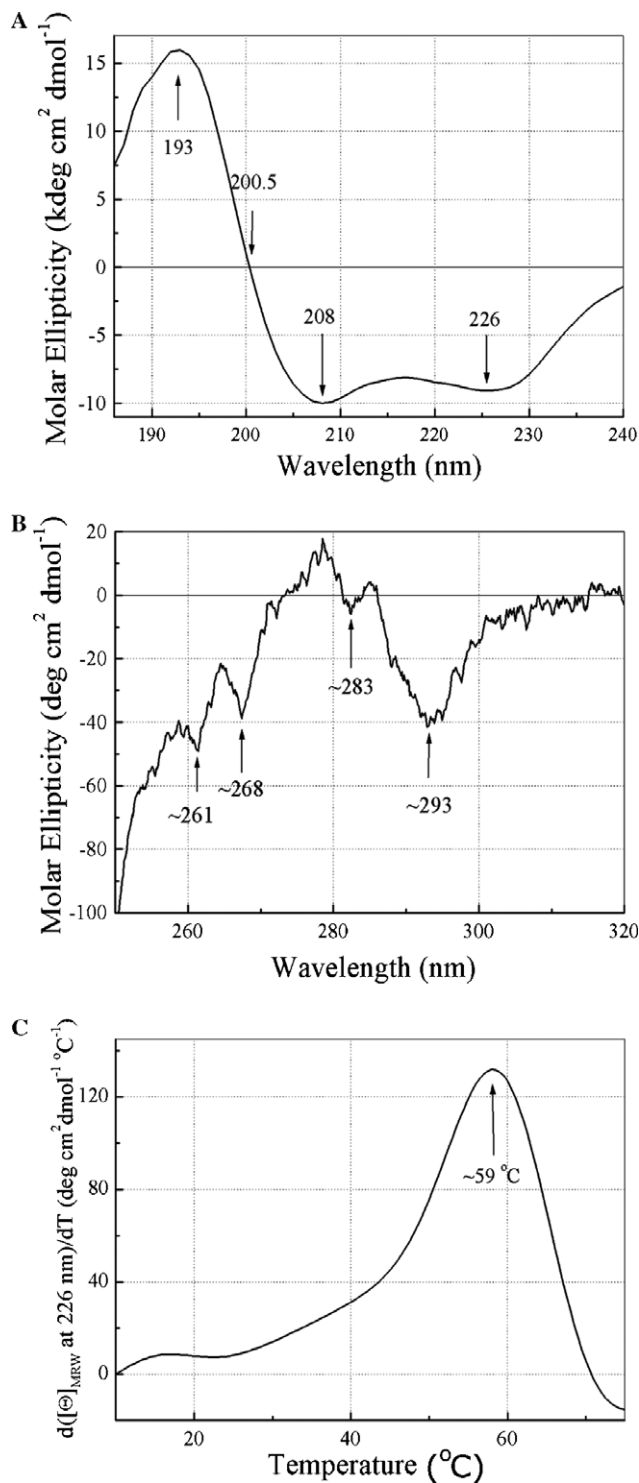


Fig. 4. CD Spectra of apo-CaSR ECD. (Panel A) Far-UV CD spectrum of apo-CaSR in 20 mM Na phosphate, 0.1 M NaCl, pH 7.2, at 10 °C. (Panel B) Near-UV CD spectrum of apo-CaSR in 20 mM Na phosphate, 0.1 M NaCl, pH 7.2, at 10 °C. (Panel C). Temperature dependence of the first derivative of mean residual weight (MRW) molar ellipticity at 226 nm for apo-CaSR in 20 mM Na phosphate, 0.1 M NaCl, pH 7.2. Arrow shows the midpoint of the melting curve.

band of TRP attributed to L_a transition is responsible for positive values of molar ellipticity in the range 274–282 nm. The presence of these peaks proves the existence

Table 1
Secondary structure^a of CaSR in apo-state at 10 °C

H (helix)	S (β strand)			Turns	Unordered
	Regular	Distorted	Total		
21.1 ± 4.0	6.7 ± 3.9	15.7 ± 2.1	36.6 ± 6.7	20.2 ± 3.3	29.4 ± 4.0
Number of helices	Number of β strands	Average length of helix	Average length of β strand	Tertiary structure class	
21.9 ± 2.9	18.4 ± 4.3	9.3 ± 0.4	3.9 ± 1.0	α + β	

^a H_{regular} or S_{regular} , fraction of residues (%) in central part of helical segments or strands; $H_{\text{distorted}}$ or $S_{\text{distorted}}$, fraction of terminus residues (%) in helices (two at each end of helix; four total per helical segment) or β strands (one residue at each end of strand, two total per strand); total, total content of H or S structure is equal to the sum of the fractions of regular and distorted residues; average length of helix or β strand, average number of residues per helix (~1.5 Å per residue) or β strand (~3.4 Å per residue).

of a rigid well-developed tertiary structure of apo-CaSR ECD.

Temperature stability

Fig. 4C shows the temperature dependence of the first derivative of mean residual weight (MRW) molar ellipticity of apo-CaSR ECD. The first derivative of temperature dependence of molar ellipticity at 226 nm consists of a single peak at ~59 °C. The heat denaturation is irreversible and at high temperatures is accompanied by formation of intermolecular or aggregational β-sheet structure (data not shown). The formal application of the Denatured Protein Analysis program gives changes of enthalpy and entropy values equal to $\Delta H = -178 \pm 4$ kJ/mol and $\Delta S = -535 \pm 13$ J/mol/K. However, the irreversibility of the heat denaturation does lead to a dependence of these values on the protein concentration and temperature scan rate.

In conclusion, we have expressed and purified a segment of the extracellular domain of the CaSR in amounts suitable for crystallography. The purified CaSR ECD is of high homogeneity and the expressed protein, unlike in a previously described method [37], is not glycosylated. The CaSR ECD binds to calcium and neomycin, forms dimers in the absence of reducing agents, and it has a well-developed tertiary structure as determined by CD spectroscopy.

References

- [1] E.M. Brown, G. Gamba, D. Riccardi, M. Lombardi, R. Butters, O. Kifor, A. Sun, M.A. Hediger, J. Lytton, S.C. Hebert, Cloning and characterization of an extracellular Ca^{2+} -sensing receptor from bovine parathyroid, *Nature* 366 (1993) 575–580.
- [2] E.M. Brown, R.J. MacLeod, Extracellular calcium sensing and extracellular calcium signaling, *Physiol. Rev.* 81 (2001) 239–297.
- [3] J. Tfelt-Hansen, P. Schwarz, E.M. Brown, N. Chattopadhyay, The calcium-sensing receptor in human disease, *Front Biosci.* 8 (2003) s377–s390.
- [4] J. Tfelt-Hansen, E.M. Brown, The calcium-sensing receptor in normal physiology and pathophysiology: a review, *Crit. Rev. Clin. Lab. Sci.* 42 (2005) 35–70.
- [5] A.M. Hofer, E.M. Brown, Extracellular calcium sensing and signaling, *Nat. Rev. Mol. Cell Biol.* 4 (2003) 530–538.
- [6] G.N. Hendy, L. D'Souza-Li, B. Yang, L. Canaff, D.E. Cole, Mutations of the calcium-sensing receptor (CASR) in familial hypocalciuric hypercalcemia, neonatal severe hyperparathyroidism, and autosomal dominant hypocalcemia, *Hum. Mutat.* 16 (2000) 281–296.
- [7] M. Ruat, M.E. Molliver, A.M. Snowman, S.H. Snyder, Calcium sensing receptor: molecular cloning in rat and localization to nerve terminals, *Proc. Natl. Acad. Sci. USA* 92 (1995) 3161–3165.
- [8] M. Ruat, A.M. Snowman, L.D. Hester, S.H. Snyder, Cloned and expressed rat Ca^{2+} -sensing receptor, *J. Biol. Chem.* 271 (1996) 5972–5975.
- [9] R. Wang, C. Xu, W. Zhao, J. Zhang, K. Cao, B. Yang, L. Wu, Calcium and polyamine regulated calcium-sensing receptors in cardiac tissues, *Eur. J. Biochem.* 270 (2003) 2680–2688.
- [10] D. Riccardi, J. Park, W.S. Lee, G. Gamba, E.M. Brown, S.C. Hebert, Cloning and functional expression of a rat kidney extracellular

- calcium/polyvalent cation-sensing receptor, *Proc. Natl. Acad. Sci. USA* 92 (1995) 131–135.
- [11] S.X. Cheng, M. Okuda, A.E. Hall, J.P. Geibel, S.C. Hebert, Expression of calcium-sensing receptor in rat colonic epithelium: evidence for modulation of fluid secretion, *Am. J. Physiol. Gastrointest Liver Physiol.* 283 (2002) G240–G250.
- [12] I. Cheng, I. Qureshi, N. Chattopadhyay, A. Qureshi, R.R. Butters, A.E. Hall, R.R. Cima, K.V. Rogers, S.C. Hebert, J.P. Geibel, E.M. Brown, D.I. Soybel, Expression of an extracellular calcium-sensing receptor in rat stomach, *Gastroenterology* 116 (1999) 118–126.
- [13] M.J. Rutten, K.D. Bacon, K.L. Marlink, M. Stoney, C.L. Meichsner, F.P. Lee, S.A. Hobson, K.D. Rodland, B.C. Sheppard, D.D. Trunkey, K.E. Deveney, C.W. Deveney, Identification of a functional Ca^{2+} -sensing receptor in normal human gastric mucous epithelial cells, *Am. J. Physiol.* 277 (1999) G662–G670.
- [14] E.F. Nemeth, Pharmacological regulation of parathyroid hormone secretion, *Curr. Pharm. Des.* 8 (2002) 2077–2087.
- [15] T.A. Craig, L.M. Benson, S.Y. Venyaminov, E.S. Klimtchuk, Z. Bajzer, F.G. Prendergast, S. Naylor, R. Kumar, The metal-binding properties of DREAM: evidence for calcium-mediated changes in DREAM structure, *J. Biol. Chem.* 277 (2002) 10955–10966.
- [16] T.A. Craig, L.M. Benson, H.R. Bergen 3rd, S.Y. Venyaminov, J.L. Salisbury, Z.C. Ryan, J.R. Thompson, J. Sperry, M.L. Gross, R. Kumar, Metal-binding properties of human centrin-2 determined by micro-electrospray ionization mass spectrometry and UV spectroscopy, *J. Am. Soc. Mass Spectrom.* (2006).
- [17] T.D. Veenstra, A.J. Tomlinson, L. Benson, R. Kumar, S. Naylor, Low temperature aqueous electrospray ionization mass spectrometry of noncovalent complexes, *J. Am. Soc. Mass Spectrom.* 9 (1998) 580–584.
- [18] M.H. Caruthers, S.L. Beaucage, J.W. Efcavitch, E.F. Fisher, M.D. Matteucci, Y. Stabinsky, New chemical methods for synthesizing polynucleotides, *Nucleic Acids Symp. Ser.* (1980) 215–223.
- [19] M.H. Caruthers, W.K. Brill, A. Grandas, Y.X. Ma, J. Nielsen, J.Y. Tang, Synthesis of oligodeoxynucleoside phosphorodithioates, *Nucleic Acids Symp. Ser.* (1989) 119–120.
- [20] M.D. Matteucci, M.H. Caruthers, Synthesis of deoxyoligonucleotides on a polymer support, 1981, *Biotechnology* 24 (1992) 92–98.
- [21] F. Sanger, S. Nicklen, A.R. Coulson, DNA sequencing with chain-terminating inhibitors, *Proc. Natl. Acad. Sci. USA* 74 (1977) 5463–5467.
- [22] M.M. Bradford, A rapid and sensitive method for the quantitation of microgram quantities of protein utilizing the principle of protein-dye binding, *Anal. Biochem.* 72 (1976) 248–254.
- [23] F.M. Ausubel, R. Brent, R.E. Kingston, D.D. Moore, J.G. Seidman, J.A. Smith, J.A. Struhl, *Current Protocols and Molecular Biology*, John Wiley and Sons, Inc, 2006.
- [24] L. Ikonomou, G. bastin, Y. Schneider, S. Agatho, Design of an efficient medium for insects cell growth and recombinant protein production, *In Vitro Cell Dev. Biol. Anim.* 287 (2001) 243–251.
- [25] K. Radika, D.B. Northrop, Purification of two forms of kanamycin acetyltransferase from *Escherichia coli*, *Arch. Biochem. Biophys.* 233 (1984) 272–285.
- [26] E.J. Mihaly, Numerical values of the absorbance is off the aromatic amino acids in acid, and neutral and alkaline solutions, *Chem. Eng. Data* 113 (1968) 179–182.
- [27] S.C. Gill, P.H. von Hippel, Calculation of protein extinction coefficients from amino acid sequence data, *Anal. Biochem.* 182 (1989) 319–326.
- [28] H. Mach, C.R. Middaugh, R.V. Lewis, Statistical determination of the average values of the extinction coefficients of tryptophan and tyrosine in native proteins, *Anal. Biochem.* 200 (1992) 74–80.
- [29] C.N. Pace, F. Vajdos, L. Fee, G. Grimsley, T. Gray, How to measure and predict the molar absorption coefficient of a protein, *Protein Sci.* 4 (1995) 2411–2423.
- [30] N. Sreerama, R.W. Woody, Estimation of protein secondary structure from circular dichroism spectra: comparison of CONTIN, SELCON, and CDSSTR methods with an expanded reference set, *Anal. Biochem.* 287 (2000) 252–260.
- [31] N. Sreerama, S.Y. Venyaminov, R.W. Woody, Estimation of the number of α -helical and β -strand segments in proteins using circular dichroism spectroscopy, *Protein Sci.* 8 (1999) 370–380.
- [32] S.W. Provencher, J. Glockner, Estimation of globular protein secondary structure from circular dichroism, *Biochemistry* 20 (1981) 33–37.
- [33] I.H. van Stokkum, H.J. Spoelder, M. Bloemendal, R. van Grondelle, F.C. Groen, Estimation of protein secondary structure and error analysis from circular dichroism spectra, *Anal. Biochem.* 191 (1990) 110–118.
- [34] W.C. Johnson, Analyzing protein circular dichroism spectra for accurate secondary structures, *Proteins* 35 (1999) 307–312.
- [35] S. Venyaminov, K.S. Vassilenko, Determination of protein tertiary structure class from circular dichroism spectra, *Anal. Biochem.* 222 (1994) 176–184.
- [36] N. Sreerama, S.Y. Venyaminov, R.W. Woody, Estimation of protein secondary structure from circular dichroism spectra: inclusion of denatured proteins with native proteins in the analysis, *Anal. Biochem.* 287 (2000) 243–251.
- [37] P.K. Goldsmith, G.F. Fan, K. Ray, J. Shiloach, P. McPhie, K.V. Rogers, A.M. Spiegel, Expression, purification, and biochemical characterization of the amino-terminal extracellular domain of the human calcium receptor, *J. Biol. Chem.* 274 (1999) 11303–11309.